Gravitational waves astronomy with LIGO and Virgo interferometers

Lazzaro Claudia
Virgo and LIGO Collaboration
Dipartimento di Fisica e Astronomia
EFT methods from Bound States to Binary Systems
Padova 28 October 2020

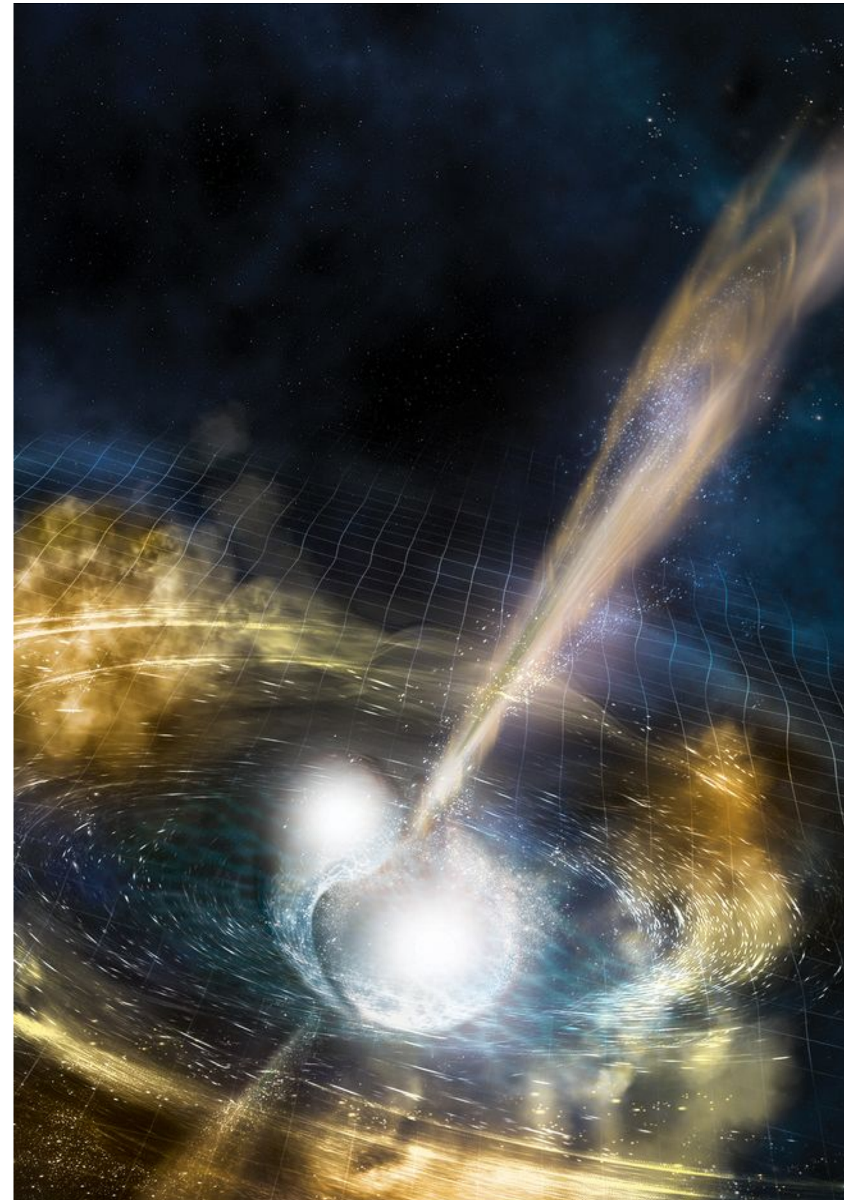

LIGO Scientific Collaboration

UNIVERSITÀ DEGLI STUDI DI PADOVA

Outline

- Interferometers network in O1 O2 O3 data taking
- GW searches results: Gravitational Wave Transient Catalog 1 (GWTC-1) and test of general relativity with GWTC-1
- GW O3 exceptional events
- future GW interferometer networks

O3 data taking

Till now 3 data taking:
O1: 12 Sep 2015 -20 Oct 2015
O2: 30 Nov 2016 - Aug 25th
O3a: 1 Apr 2019 - 1 Oct 2019
O3b: 1 Nov 2019 - 27 Mar 2020
O3b data taking ended due to the impact of COVID-19

Duty cycle of the interferometer network

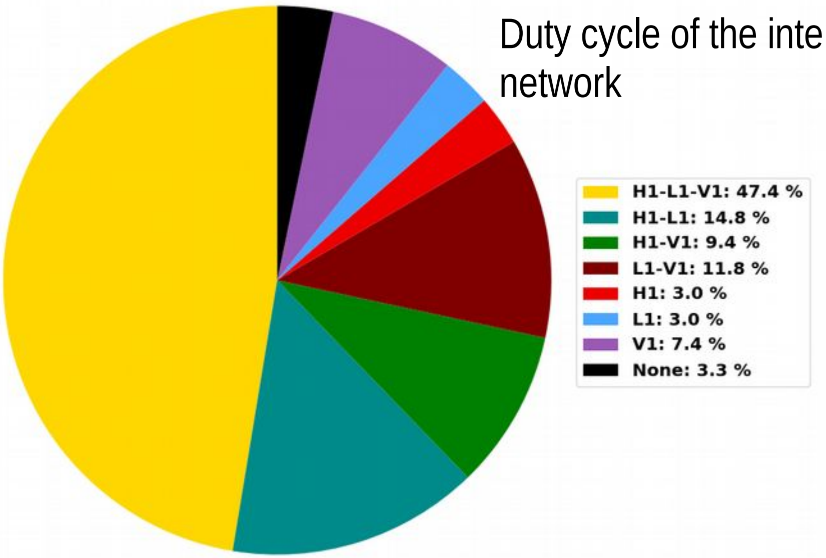

The sensitivity, quantified by Binary neutron start inspiral range for first phase of O3:

- Hanford: 102–111 Mpc
- Livigstone 125–140 Mpc
- Virgo: 43– 50 Mpc over the fi rst three months of O3 (improved in the last part of the run)

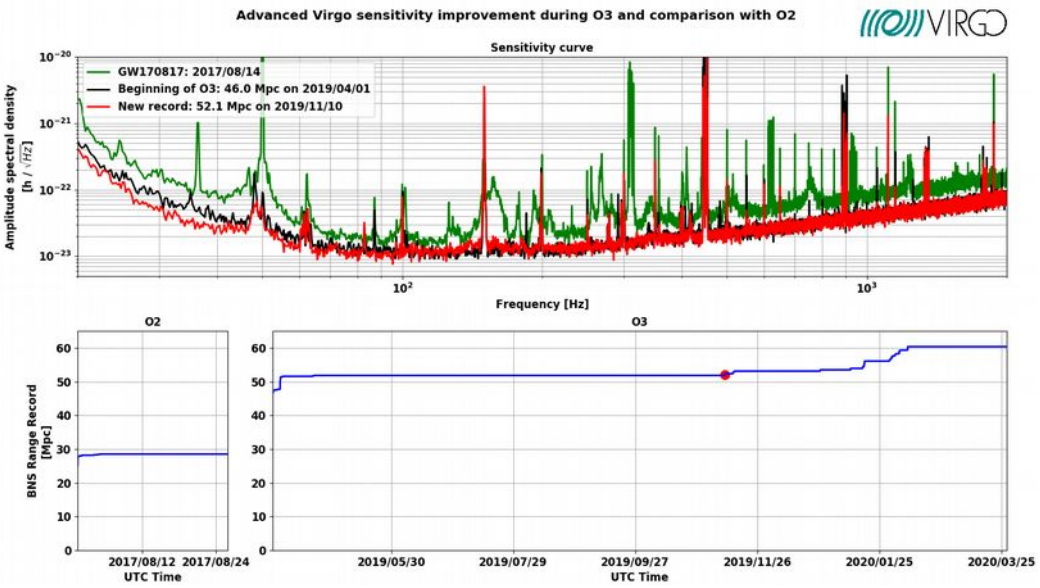

https://www.virgo-gw.eu/status.html

O1-O2-O3 data taking

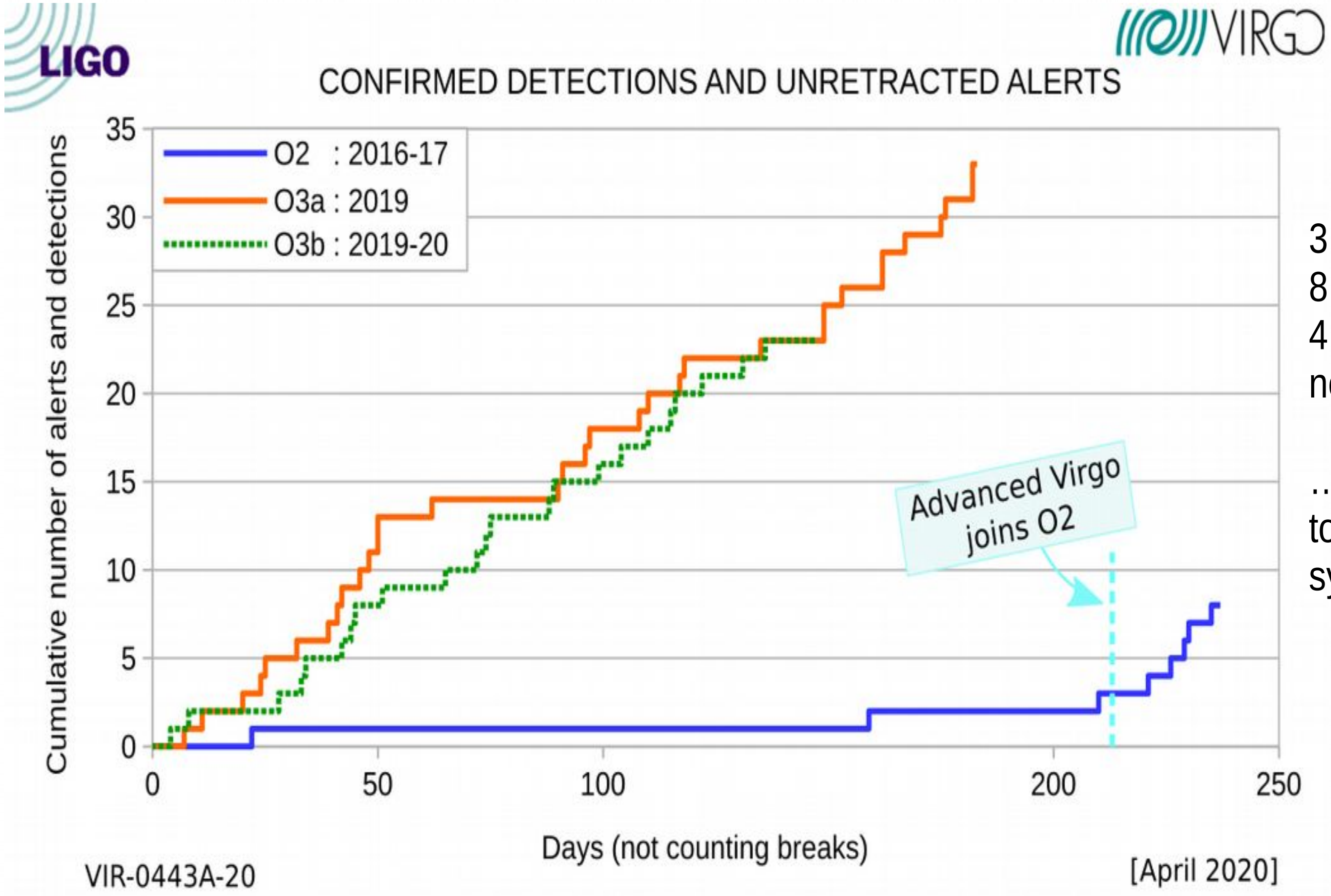

3 GW signals detected in O1
8 GW signals detected in O2
4 GW signals detected and published till now in O3

… all detections (published till now) due to coalescence in compact binary systems

https://www.virgo-gw.eu/status.html

Gravitational-wave Transient Catalog-1

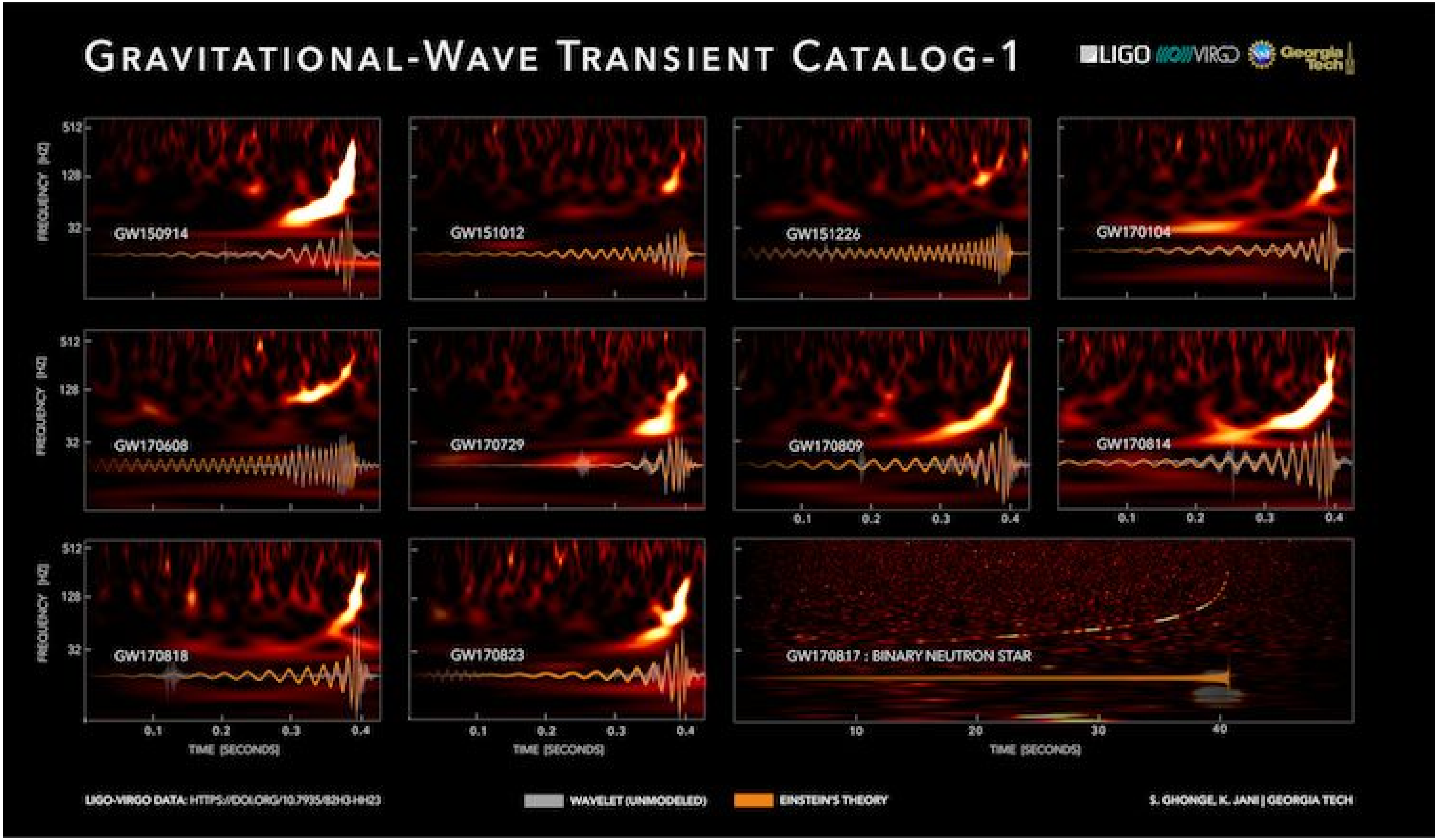

Compact binary coalescence searches for O1&O2 data taking: Physical review X 9, 031040 (2019)

Waveforms

Two body problem in general relativity solved:
approximately, but analytically
exactly, but numerically

Analytical methods: post-Newtonian/post-Minkowskian and effective-one-body theory

models are built by combining post-Newtonian calculations the effective-one-body formalism and numerical relativity

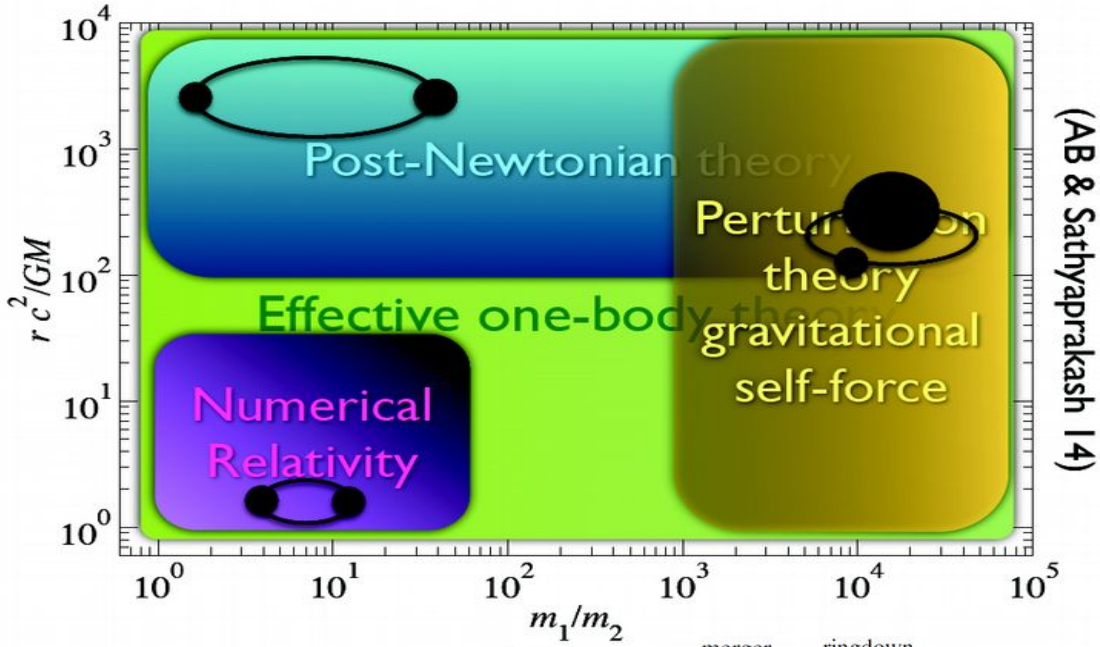

Properties of the binary systems (masses, spins, precession...) are extracted from gravitational waves via Bayesian inference by using theoretical models
Binary black hole system: inspiral, merger, and ringdown of the final object
Binary neutron stars system: inspiral and merger

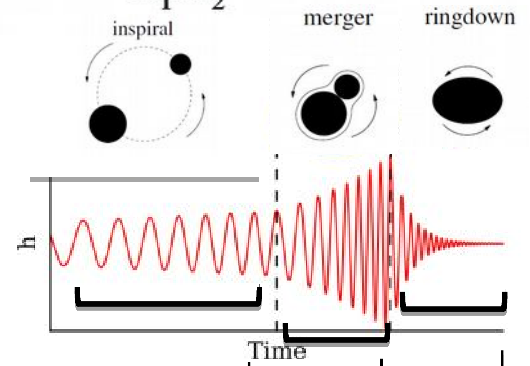

post-Newtonian (PN) theory

numerical solution available

ringdown perturbation theory or numerical solution available

GWTC-1: detection significance

Cumulative histograms of search results vs inverse false-alarm rate (dashed: expected background, shaded regions: sigma uncertainty bounds for Poisson uncertainty, blue dots are the named gravitational-wave events found

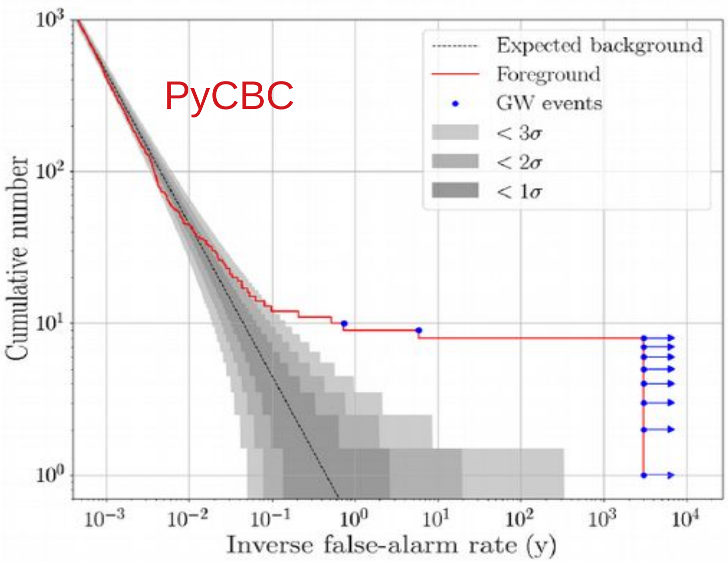

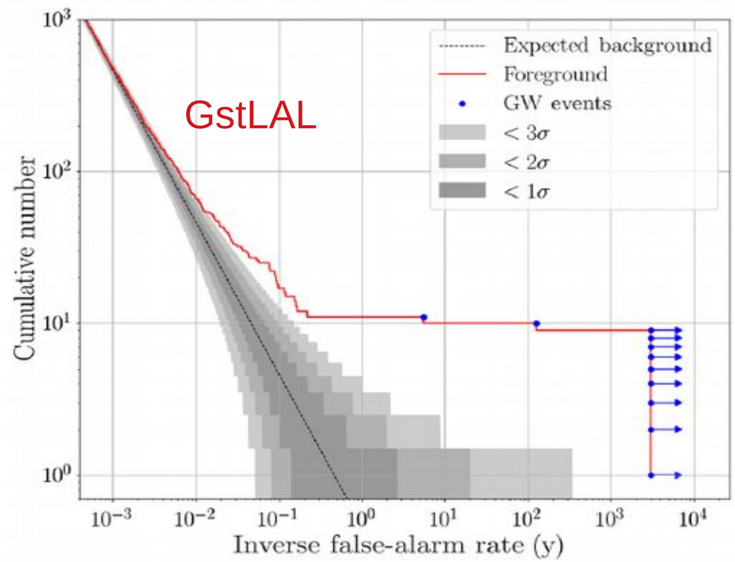

Templated searches:
matched filter using bank of templates to cover the parameter space

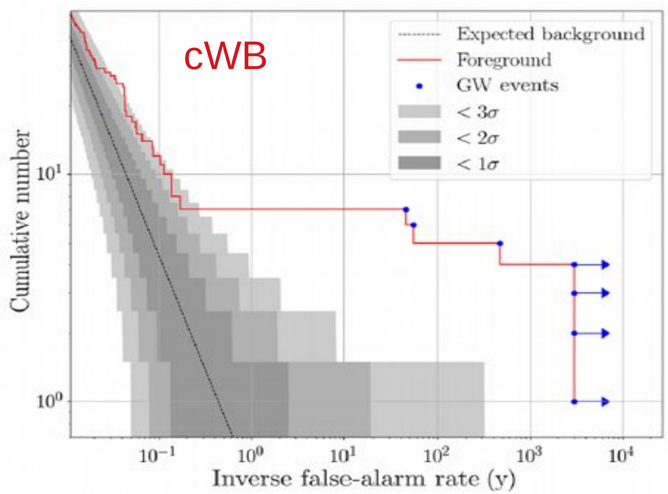

Model independent searches:

- search of excess power in the time frequency representation of interferometers network data
- Likelihood approach to reconstruct coherent signal through the interferometers

GWTC-1

Event	$m_1/M_\odot$	$m_2/M_\odot$	$\mathcal{M}/M_\odot$	$\chi_{\rm eff}$	$M_f/M_\odot$	a_f	$E_{\rm rad}/(M_\odot c^2)$	$\ell_{\rm peak}/({\rm erg\,s^{-1}})$	$d_L/{\rm Mpc}$	z	$\Delta\Omega/{\rm deg}^2$
GW150914	$35.6^{+4.7}_{-3.1}$	$30.6^{+3.0}_{-4.4}$	$28.6^{+1.7}_{-1.5}$	$-0.01^{+0.12}_{-0.13}$	$63.1^{+3.4}_{-3.0}$	$0.69^{+0.05}_{-0.04}$	$3.1^{+0.4}_{-0.4}$	$3.6^{+0.4}_{-0.4}\times10^{56}$	440^{+150}_{-170}	$0.09^{+0.03}_{-0.03}$	182
GW151012	$23.2^{+14.9}_{-5.5}$	$13.6^{+4.1}_{-4.8}$	$15.2^{+2.1}_{-1.2}$	$0.05^{+0.31}_{-0.20}$	$35.6^{+10.8}_{-3.8}$	$0.67^{+0.13}_{-0.11}$	$1.6^{+0.6}_{-0.5}$	$3.2^{+0.8}_{-1.7}\times10^{56}$	1080^{+550}_{-490}	$0.21^{+0.09}_{-0.09}$	1523
GW151226	$13.7^{+8.8}_{-3.2}$	$7.7^{+2.2}_{-2.5}$	$8.9^{+0.3}_{-0.3}$	$0.18^{+0.20}_{-0.12}$	$20.5^{+6.4}_{-1.5}$	$0.74^{+0.07}_{-0.05}$	$1.0^{+0.1}_{-0.2}$	$3.4^{+0.7}_{-1.7}\times10^{56}$	450^{+180}_{-190}	$0.09^{+0.04}_{-0.04}$	1033
GW170104	$30.8^{+7.3}_{-5.6}$	$20.0^{+4.9}_{-4.6}$	$21.4^{+2.2}_{-1.8}$	$-0.04^{+0.17}_{-0.21}$	$48.9^{+5.1}_{-4.0}$	$0.66^{+0.08}_{-0.11}$	$2.2^{+0.5}_{-0.5}$	$3.3^{+0.6}_{-1.0}\times10^{56}$	990^{+440}_{-430}	$0.20^{+0.08}_{-0.08}$	921
GW170608	$11.0^{+5.5}_{-1.7}$	$7.6^{+1.4}_{-2.2}$	$7.9^{+0.2}_{-0.2}$	$0.03^{+0.19}_{-0.07}$	$17.8^{+3.4}_{-0.7}$	$0.69^{+0.04}_{-0.04}$	$0.9^{+0.0}_{-0.1}$	$3.5^{+0.4}_{-1.3}\times10^{56}$	320^{+120}_{-110}	$0.07^{+0.02}_{-0.02}$	392
GW170729	$50.2^{+16.2}_{-10.2}$	$34.0^{+9.1}_{-10.1}$	$35.4^{+6.5}_{-4.8}$	$0.37^{+0.21}_{-0.25}$	$79.5^{+14.7}_{-10.2}$	$0.81^{+0.07}_{-0.13}$	$4.8^{+1.7}_{-1.7}$	$4.2^{+0.9}_{-1.5}\times10^{56}$	2840^{+1400}_{-1360}	$0.49^{+0.19}_{-0.21}$	1041
GW170809	$35.0^{+8.3}_{-5.9}$	$23.8^{+5.1}_{-5.2}$	$24.9^{+2.1}_{-1.7}$	$0.08^{+0.17}_{-0.17}$	$56.3^{+5.2}_{-3.8}$	$0.70^{+0.08}_{-0.09}$	$2.7^{+0.6}_{-0.6}$	$3.5^{+0.6}_{-0.9}\times10^{56}$	1030^{+320}_{-390}	$0.20^{+0.05}_{-0.07}$	308
GW170814	$30.6^{+5.6}_{-3.0}$	$25.2^{+2.8}_{-4.0}$	$24.1^{+1.4}_{-1.1}$	$0.07^{+0.12}_{-0.12}$	$53.2^{+3.2}_{-2.4}$	$0.72^{+0.07}_{-0.05}$	$2.7^{+0.4}_{-0.3}$	$3.7^{+0.4}_{-0.5}\times10^{56}$	600^{+150}_{-220}	$0.12^{+0.03}_{-0.04}$	87
GW170817	$1.46^{+0.12}_{-0.10}$	$1.27^{+0.09}_{-0.09}$	$1.186^{+0.001}_{-0.001}$	$0.00^{+0.02}_{-0.01}$	≤ 2.8	≤ 0.89	≥ 0.04	$\geq 0.1\times10^{56}$	40^{+7}_{-15}	$0.01^{+0.00}_{-0.00}$	16
GW170818	$35.4^{+7.5}_{-4.7}$	$26.7^{+4.3}_{-5.2}$	$26.5^{+2.1}_{-1.7}$	$-0.09^{+0.18}_{-0.21}$	$59.4^{+4.9}_{-3.8}$	$0.67^{+0.07}_{-0.08}$	$2.7^{+0.5}_{-0.5}$	$3.4^{+0.5}_{-0.7}\times10^{56}$	1060^{+420}_{-380}	$0.21^{+0.07}_{-0.07}$	39
GW170823	$39.5^{+11.2}_{-6.7}$	$29.0^{+6.7}_{-7.8}$	$29.2^{+4.6}_{-3.6}$	$0.09^{+0.22}_{-0.26}$	$65.4^{+10.1}_{-7.4}$	$0.72^{+0.09}_{-0.12}$	$3.3^{+1.0}_{-0.9}$	$3.6^{+0.7}_{-1.1}\times10^{56}$	1940^{+970}_{-900}	$0.35^{+0.15}_{-0.15}$	1666

LHV network

- detected 10 binary black holes have total masses between $18.6^{+3.2}_{-0.7}\,M_\odot$ and $84.4^{+15.8}_{-11.1}\,M_\odot$ and range in distance between 320^{+120}_{-110} and 2840^{+1400}_{-1360} Mpc.
- GW170817: first binary neutron star detected
- No neutron star–black hole mergers were detected.
- approximately one gravitational-wave detection per 15 days of data searched, merger rates inferred (90% confidence intervals): 110 − 3840 $\mathrm{Gpc^{-3}y^{-1}}$ for binary neutron stars and 9.7−101 $\mathrm{Gpc^{-3}y^{-1}}$ for binary black holes assuming fixed population distributions

GWTC-1

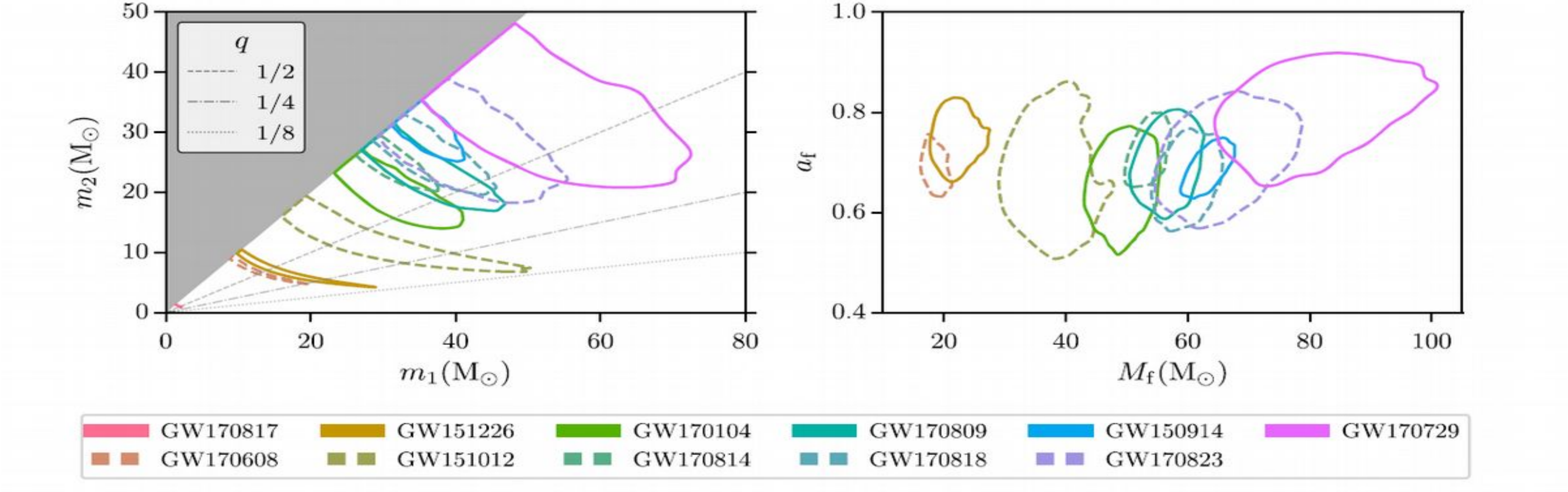

Posterior probability densities of the component masses and final masses and spins (contours show 90% credible regions)

Further works show that systematics due to modeling are smaller than statistical errors (GW150914 arXiv:1611.07531)

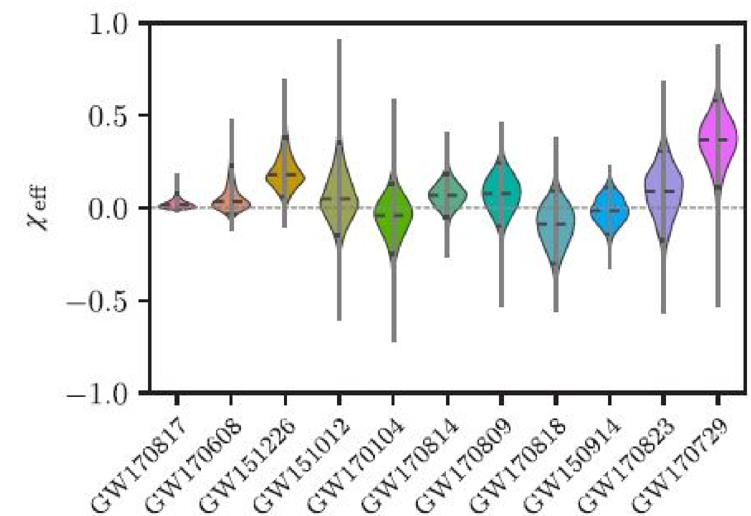

$$\chi_{\mathrm{eff}} = \frac{(m_1\vec{\chi}_1 + m_2\vec{\chi}_2)\cdot\hat{L}_N}{M}$$

GTCW-1: testing general relativity

Phys. Rev. D 100, 104036 (2019)

Four tests to determine consistency of the data with binary black hole gravitational waveforms predicted by general relativity:

✗ subtractions of the best-fit waveform from the data and checks the consistency of the residual with detector noise.

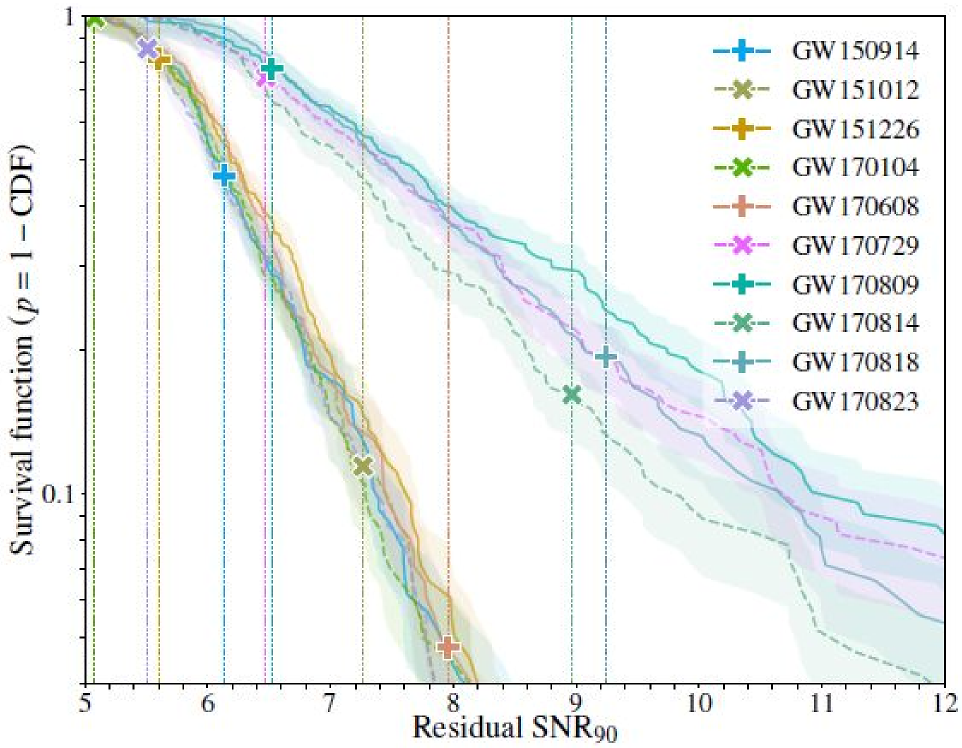

The coherent SNR using model independent BayesWaves algorithm is calculated after subtracting best waveform model to the data (1sec window)

To evaluate the obtained residual SNR consistency with detector noise: Bayes Wave analysis is performed on 200 event sets of noise-only detector data near each event → p-value for the null hypothesis

→ residuals are consistent with noise.

GTCW-1: testing general relativity

Phys. Rev. D 100, 104036 (2019)

Four tests to determine consistency of the data with binary black hole gravitational waveforms predicted by general relativity:

- ✗ subtractions of the best-fit waveform from the data and checks the consistency of the residual with detector noise.
- ✗ consistency of the low (inspiral part of the signal) and high-frequency (post inspiral) parts of the observed signals.

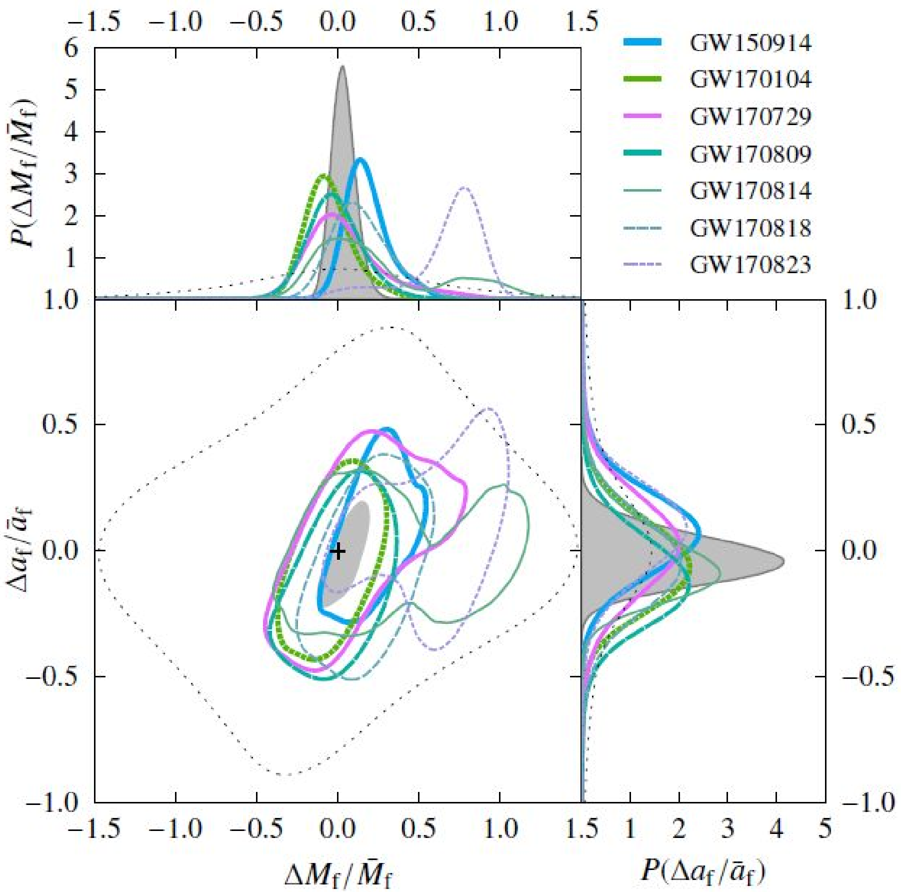

dimensionless quantities are defined to quantify the fractional difference between final black hole's mass and spin estimated from the inspiral only and post-inspiral parts of the signal.

GTCW-1: testing general relativity

Phys. Rev. D 100, 104036 (2019)

Four tests to determine consistency of the data with binary black hole gravitational waveforms predicted by general relativity:

- subtractions of the best-fit waveform from the data and checks the consistency of the residual with detector noise.
- consistency of the low (inspiral part of the signal) and high-frequency (post inspiral) parts of the observed signals.
- check phenomenological deviations introduced in the waveform model (including in the post-Newtonian coefficients) are consistent with zero.
- constrains modifications to the propagation of gravitational waves due to a modified dispersion relation

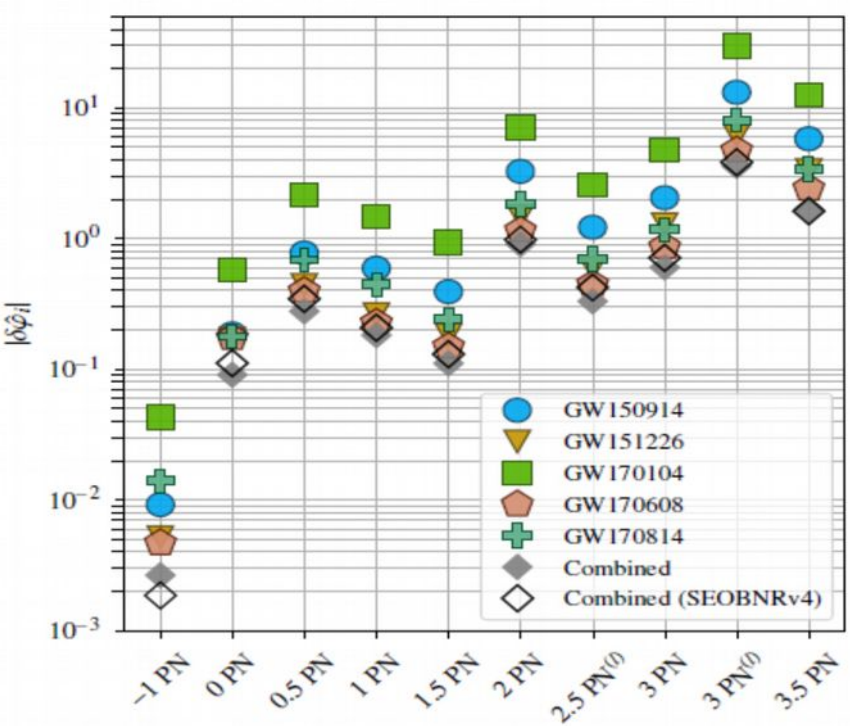

The early inspiral of compact binaries is well modeled by the post-Newtonian (PN) approximation to GR → Deviations from the GR binary dynamics are parametrized introducing shifts in each of the individual GW phase coefficients;

90% upper bounds on the absolute magnitude of the GR violating parameters (-1PN to 3.5PN) in the inspiral phase. At each PN order. Bounds obtained from combining posteriors of events detected with a significance that exceeds a threshold of FAR < (1000 yr)

These tests of GR in the highly relativistic, nonlinear regime of strong gravity, do not reveal any inconsistency of our data with the predictions of GR

GTCW-1: GW170817

Low spin prior

Phys. Rev. Lett. 119, 161101 (2017)
Phys. Rev. Lett. 121, 161101 (2018)

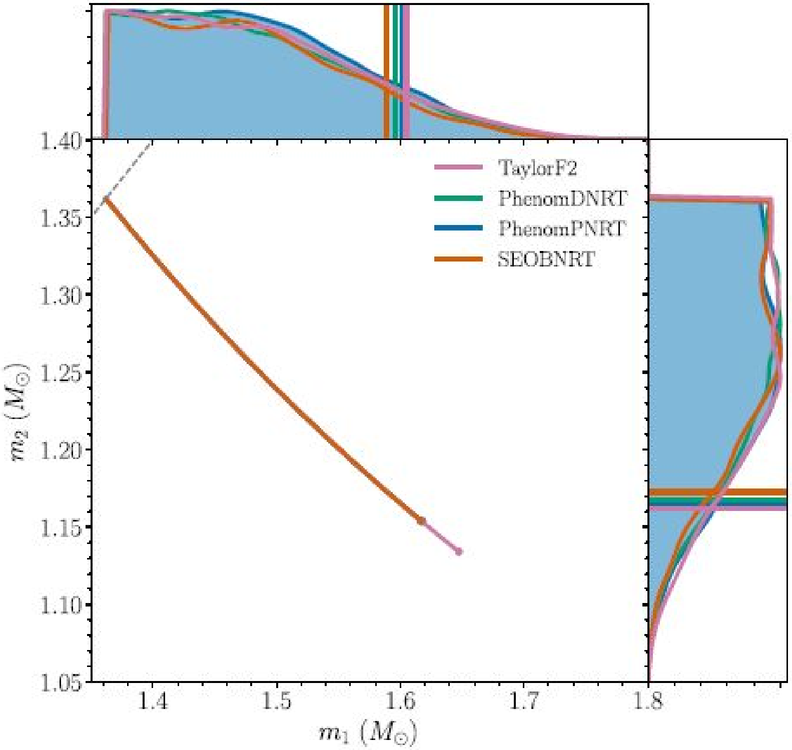

- first observation of a binary neutron star inspiral, SNR 32.4
- component masses lie in range [1.00,1.89] $M_\odot$ when allowing large component spins and lie in range [1.16, 1.60] $M_\odot$ when allowing low component spins
- Electromagnetic counterparts observations

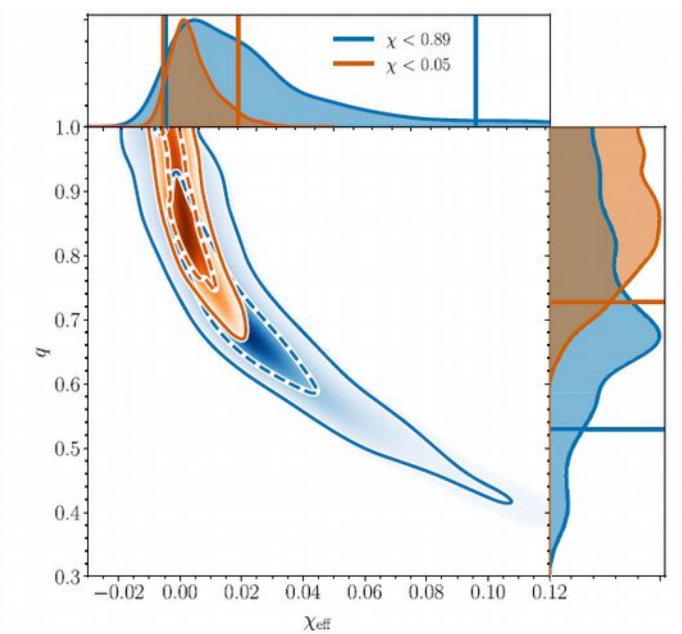

Marginalized two-dimensional posteriors for the effective spin χ_{eff} and mass ratio q using the PhenomPNRT model for the high-spin prior (blue) and low-spin prior (orange).

no evidence for nonzero component spins

GTCW-1: GW170817

Phys. Rev. Lett. 119, 161101 (201
Phys. Rev. Lett. 121, 161101 (201

BNS waveform differ from BBH inspiral phase: well described by post Newtonian approximation + tidals deformation (tides make gravitational interaction more attractive) not the case for post-merger oscillations

Credits: P. Schmidt; NR data: T. Dietrich

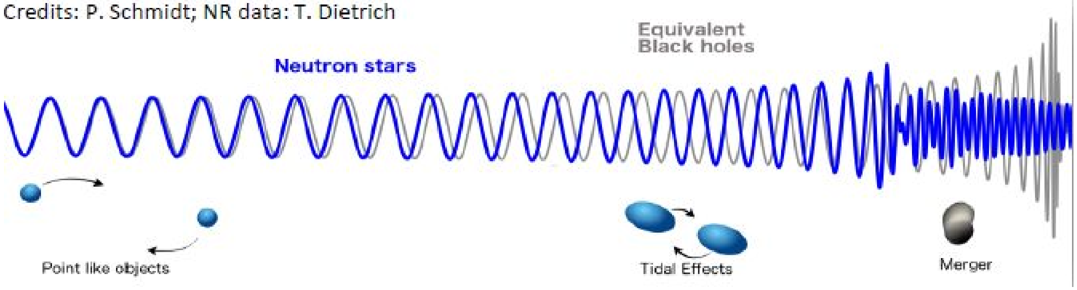

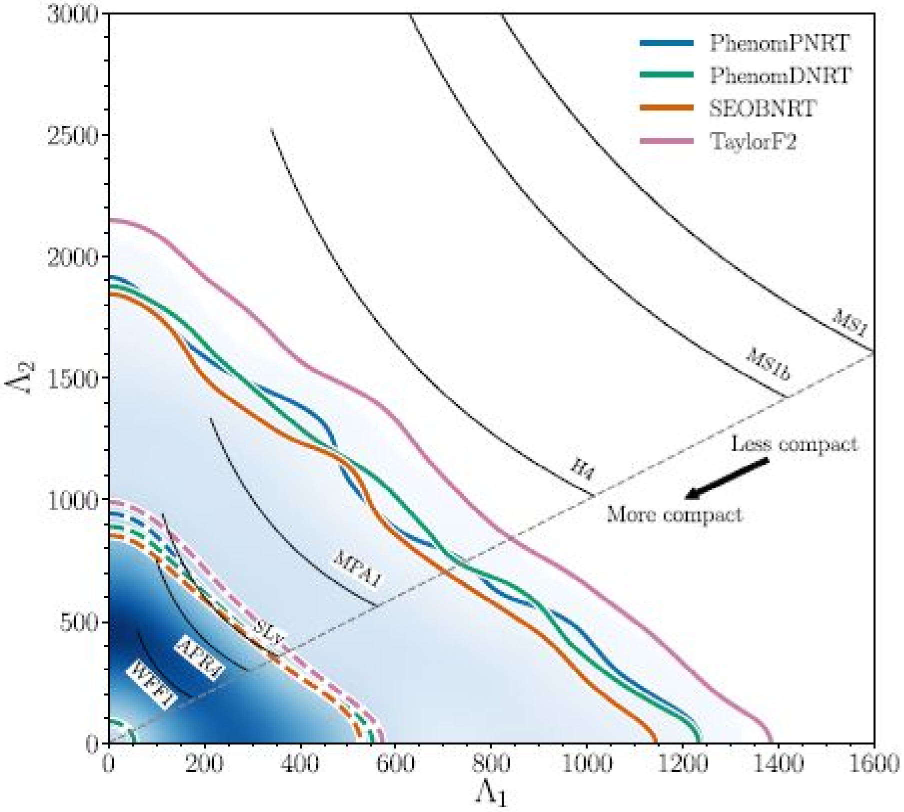

Tidal effects imprinted on gravitational waveform during inspiral phase, thought tidal deformability Λ

$\Lambda=(2/3)k_2[(c^2/G)(R/m)]^5$
K_2= second Love number
R stellar radius

- Some stiffer EOS are disfavored.
- Comparing results (on different parameters) from four different waveform models provides assurance that systematic uncertainties are small compared to statistical uncertainties.

O3 exceptional events: GW190412

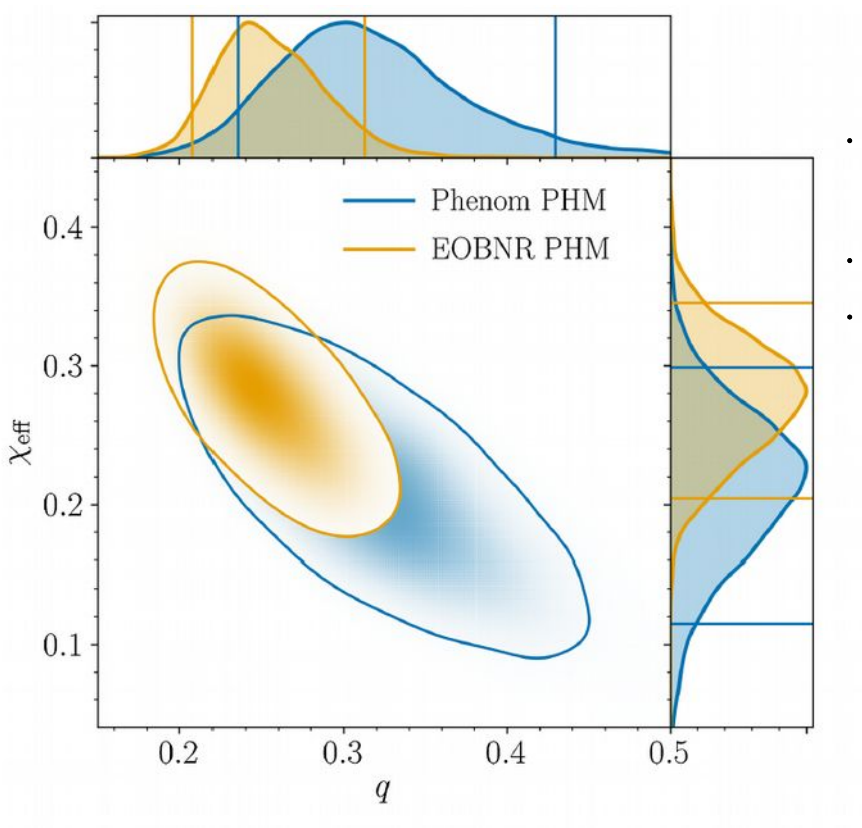

Phys. Rev. D 102, 043015 (2020)

- First GW signal observed due to coalescences of two BH with asymmetric masses of $30.1^{+4.6}_{-5.3}\,M_\odot$ and $8.3^{+1.6}_{-0.9}\,M_\odot$ black.
- Mass ratio $q = 0.28^{+0.12}_{-0.07}$ (median and 90% confidence intervals)
- Asymmetric systems are predicted to emit gravitational waves with stronger contributions from higher multipoles

The two polarization h_+ h_x of GW can be expanded into multipole moments using spherical harmonic functions:

- in case of non spinning equal mass h_{22} is (m=2) the dominant ones
- In case of unequal mass mode m=3 becomes important

O3 exceptional events: GW190412

Phys. Rev. D 102, 043015 (2020)

To estimate parameter of the BBH system:

- Models employed: SEOBNRv4PHM and IMRPhenomPv3HM include effects of higher multipoles in precessing models. EOB: inspiral-merger-ringdown (PN, black-hole perturbation theory and numerical relativity)
- Two models report posteriors distributions which are largely overlapping, but differences are visible (model depending)

→ for the first time systematic model differences are not much smaller than statistical uncertainties

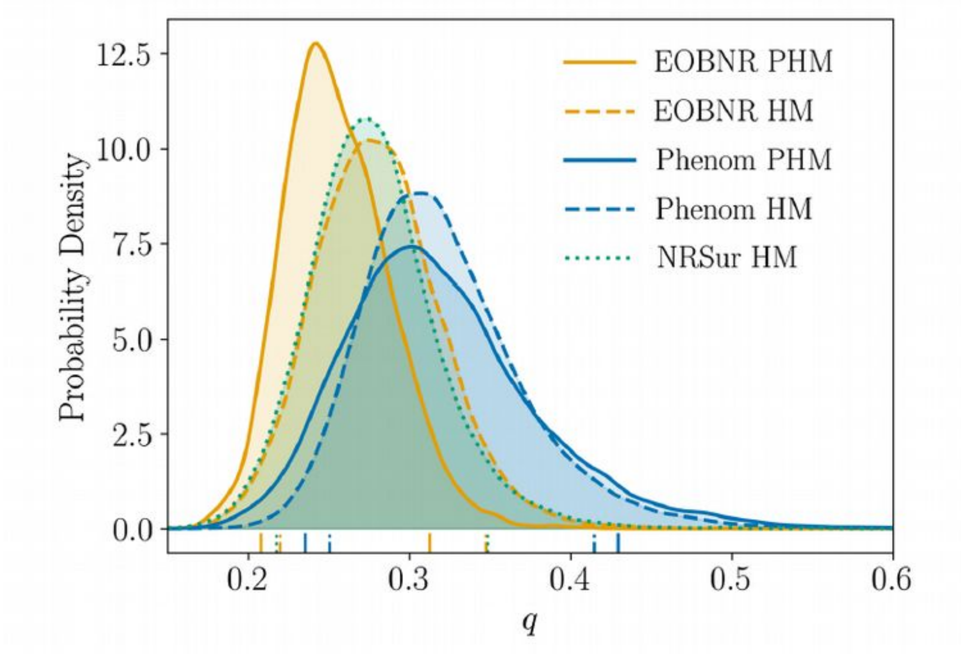

Mass-ratio measurement of GW190412 is robust against modeling systematics

O3 exceptional events: GW190412

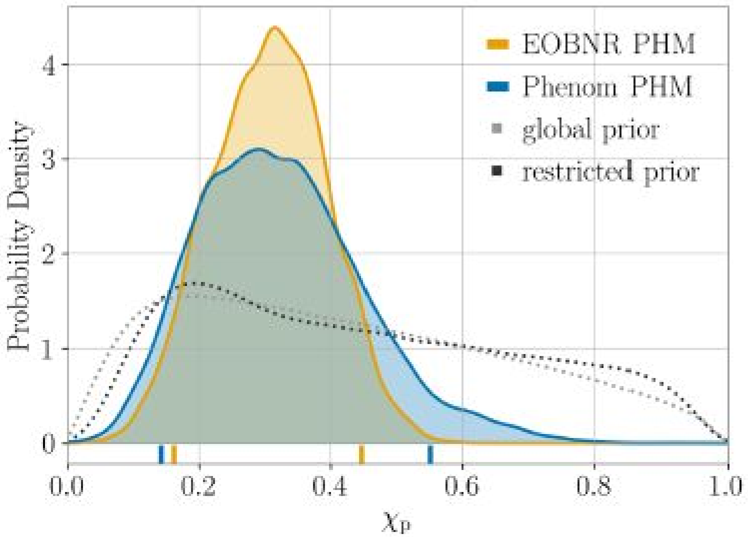

Phys. Rev. D 102, 043015 (2020)

- X_{eff} $0.25^{+0.08}_{-0.11}$ third BH binary identified with at least one non zero spin component
- X_p [0.15,0.50] at 90% credible bounds: small values X_p (<0.1) disfavored

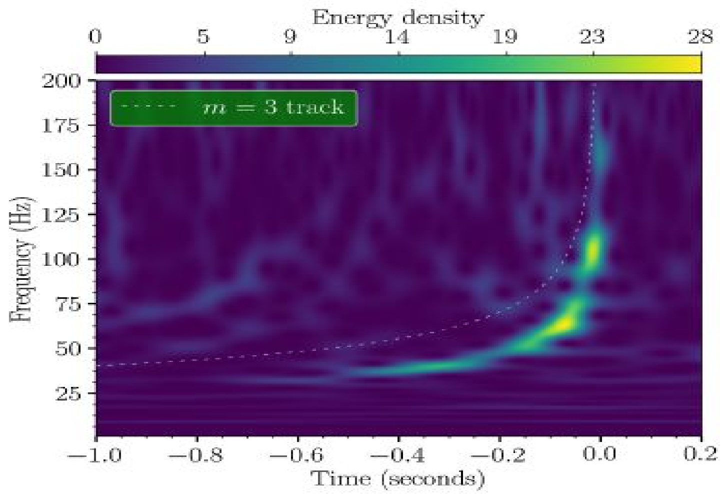

Higher multipoles:

- Many different statistical tests, all support existence of higher multipoles
- Time-frequency track methods: GW instantaneous frequency $f_{ml}(t)$ is related to the dominant mode one: $f_{ml}(t)= (m/2)f_{22}(t)$, search of “secondary” track in the time frequency representation, looking to the energy along each track $f_\alpha(t)$

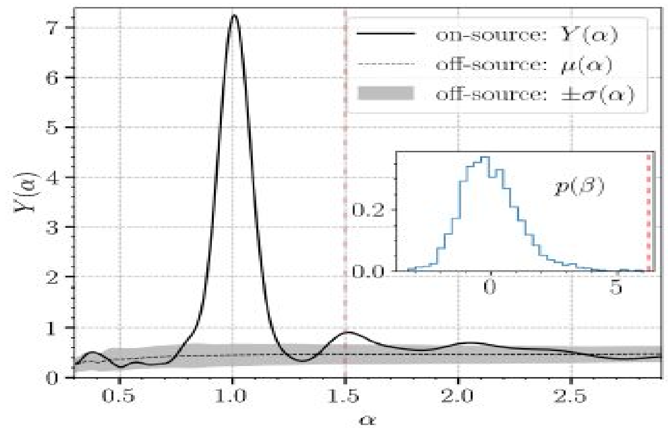

O3 exceptional events: GW190814

Astrophys. J. Lett. 896, L44 (2020)

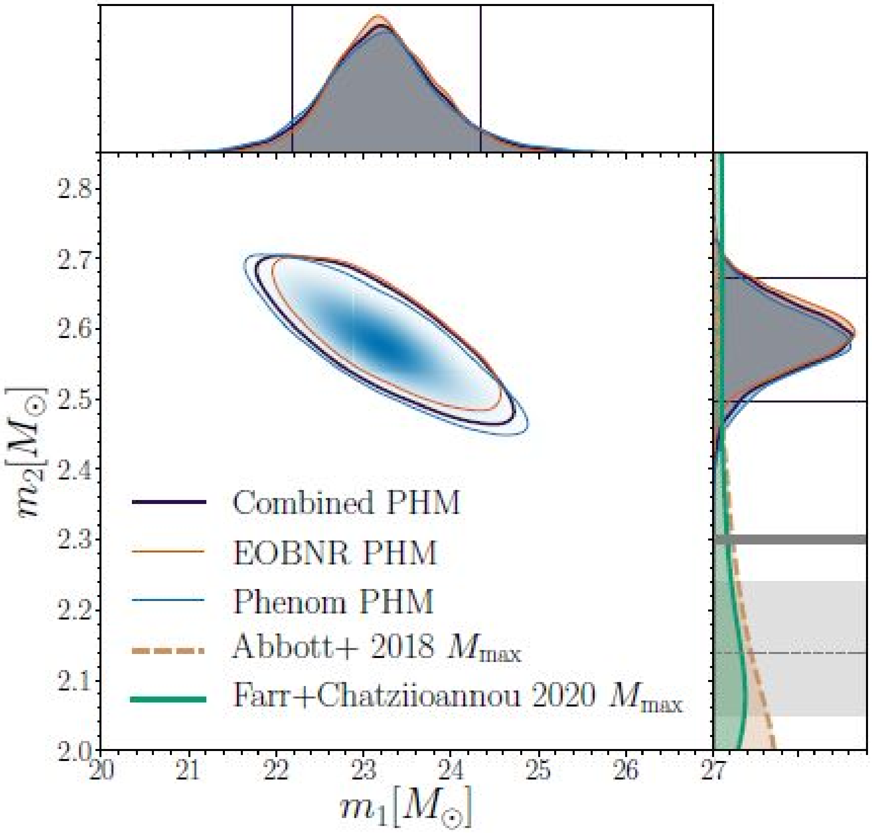

- Livingstone-Hanford-Virgo observation with SNR of 25
- Masses in the range respectively: 22.2- 24.3 $M_\odot$ and 2.50- 2.67$M_\odot$ (90% credible level)
- secondary component is either the lightest black hole or the heaviest neutron star ever discovered in a double compact-object system
- mass ratio of q = $0.112^{+0.008}_{-0.009}$ (most unequal ever observed with GW)
- The dimensionless spin of the primary black hole is constrained to <0.07
- no electromagnetic counterpart

- Tests of general relativity reveal no measurable deviations from the theory
- prediction of higher-multipole emission is confirmed at high confidence
- Comparisons between the secondary mass and estimates of the maximum NS mass suggest that this signal is unlikely to originate in a NSBH coalescence.

O3 exceptional events: GW190425

Astrophys. J. Lett. 892, L3 (2020)

	Low-spin Prior ($\chi < 0.05$)	High-spin Prior ($\chi < 0.89$)
Primary mass m_1	1.60–1.87 $M_\odot$	1.61–2.52 $M_\odot$
Secondary mass m_2	1.46–1.69 $M_\odot$	1.12–1.68 $M_\odot$
Chirp mass $\mathcal{M}$	$1.44^{+0.02}_{-0.02}$ $M_\odot$	$1.44^{+0.02}_{-0.02}$ $M_\odot$
Detector-frame chirp mass	$1.4868^{+0.0003}_{-0.0003}$ $M_\odot$	$1.4873^{+0.0008}_{-0.0006}$ $M_\odot$
Mass ratio m_2/m_1	0.8 – 1.0	0.4 – 1.0
Total mass $m_{\rm tot}$	$3.3^{+0.1}_{-0.1}$ $M_\odot$	$3.4^{+0.3}_{-0.1} M_\odot$
Effective inspiral spin parameter $\chi_{\rm eff}$	$0.012^{+0.01}_{-0.01}$	$0.058^{+0.11}_{-0.05}$
Luminosity distance $D_{\rm L}$	159^{+69}_{-72} Mpc	159^{+69}_{-71} Mpc
Combined dimensionless tidal deformability $\tilde{\Lambda}$	$\leqslant$600	$\leqslant$1100

- LIGO Livingstone detector observation of a compact binary coalescence SNR 12.9. (The Virgo detector used for parameter estimation)
- component masses range from 1.12 to 2.52 $M_\odot$, consistent with the individual binary components being neutron stars., source-frame chirp mass and the total mass are significantly larger than those of known binary BNS system.
- The possibility that one or both binary components are black holes cannot be ruled out
- Constraints on tides, radius, possible p–g instabilities and the EoS are consistent with those obtained from GW170817 (GW190425 is less constraining of NS properties)
- no clear detection of a counterpart has been reported (broad sky position region)

O3 exceptional events: GW190521

Phys. Rev. Lett. 125, 101102 (2020)

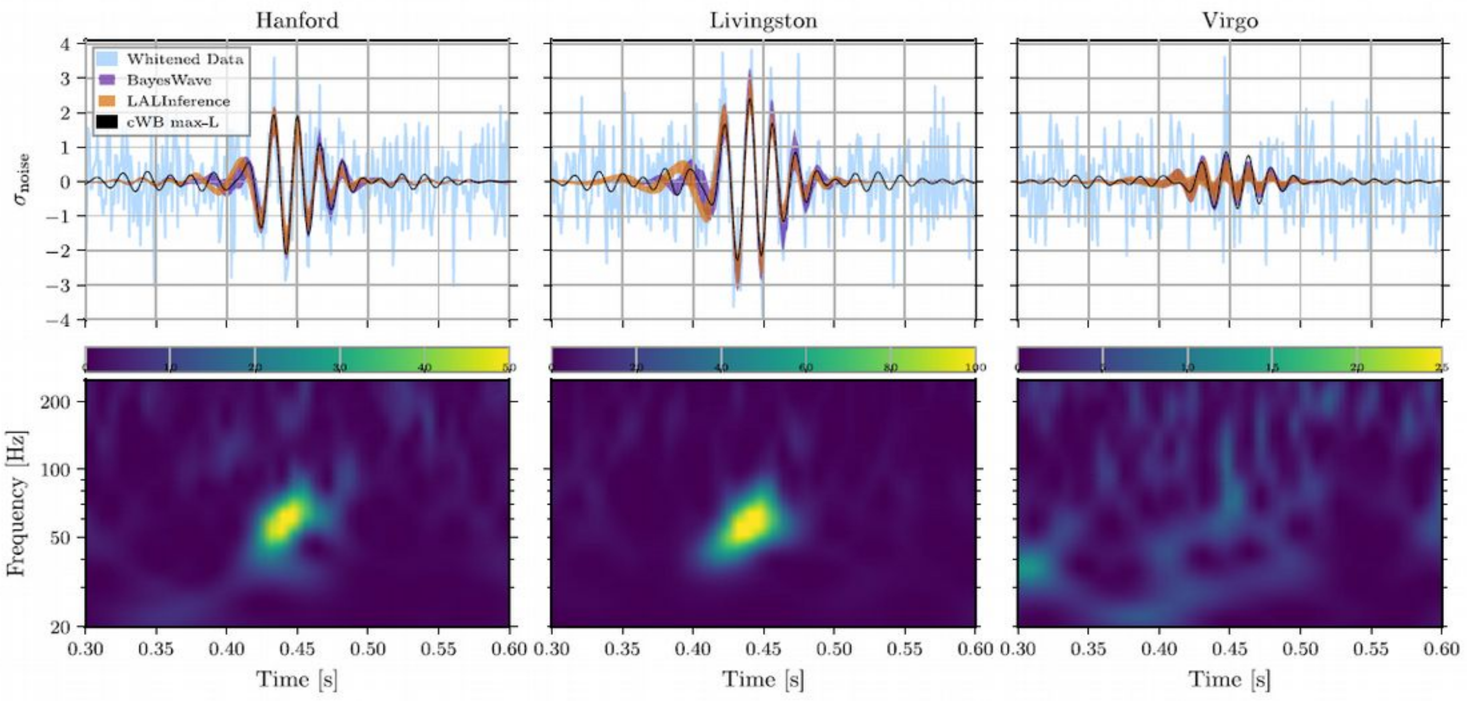

- short duration (few observable cycles) GW, three-detector network SNR: of 14.7
- estimated false-alarm rate of 1 in 4900 yr using cWB (indipendetn model search) and of 1 in 829y and 1 in 0.94y by template searches GstLAL and PyCBC (using bank of quasicircular quadrupolar mode-only non precessing templates)
- BH masses of 85^{+21}_{-14} M⊙ and 66^{+17}_{-18} $M_\odot$ (heavier in PISN mass gap)
- BH remnant mass 142^{+28}_{-16} $M_\odot$ (direct observation of formation of a IMBH)

GW190521

Phys. Rev. Lett. 125, 101102 (20

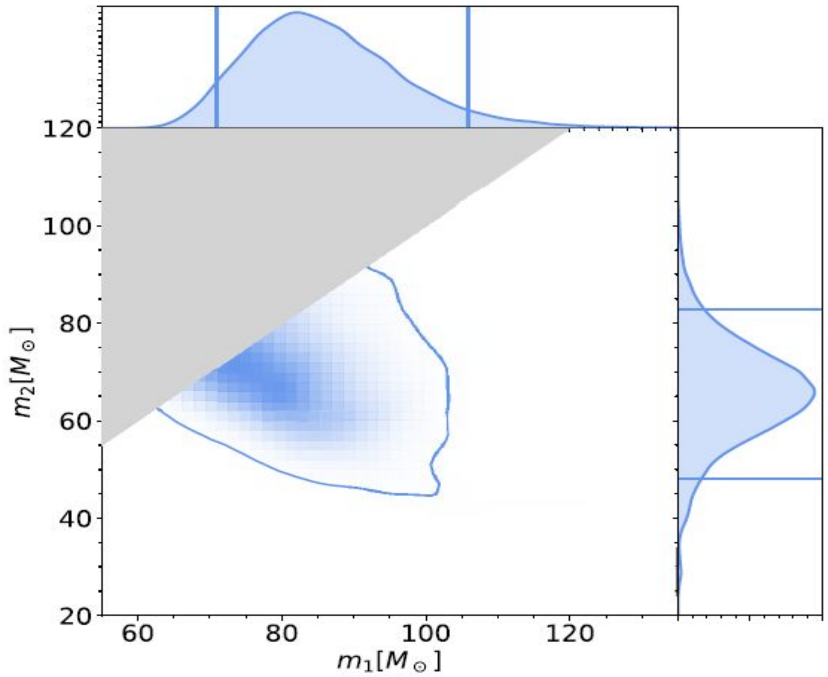

- Parameter estimation using three waveform models including higher order multiple moments and precessions (numerical relativity surrogate models NRSur7dq4, effective one body model SEOBNRv4PHM and phenomenological model IMRPhenomPv3HM
- Posterior distribution for remnant BH mass shows no support below $100M_\odot$

- Effective inspiral spin parameters χ_{eff} (spin components aligned with the orbital angular momentum) is estimated to be $0.08^{+0.27}_{-0.36}$ and effective precession spin parameters χ_p to be $0.68^{+0.25}_{-0.37}$
- Weak evidence for spinning BBH and precessing orbital plane obtained performing bayesian model selection including models omitting precession and spins
- No evidence for higher order modes

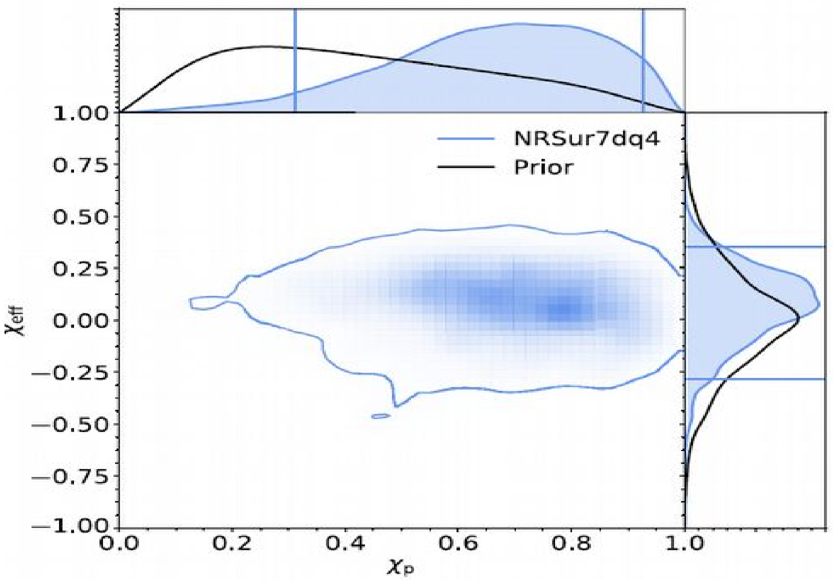

GW190521

Phys. Rev. Lett. 125, 101102 (20

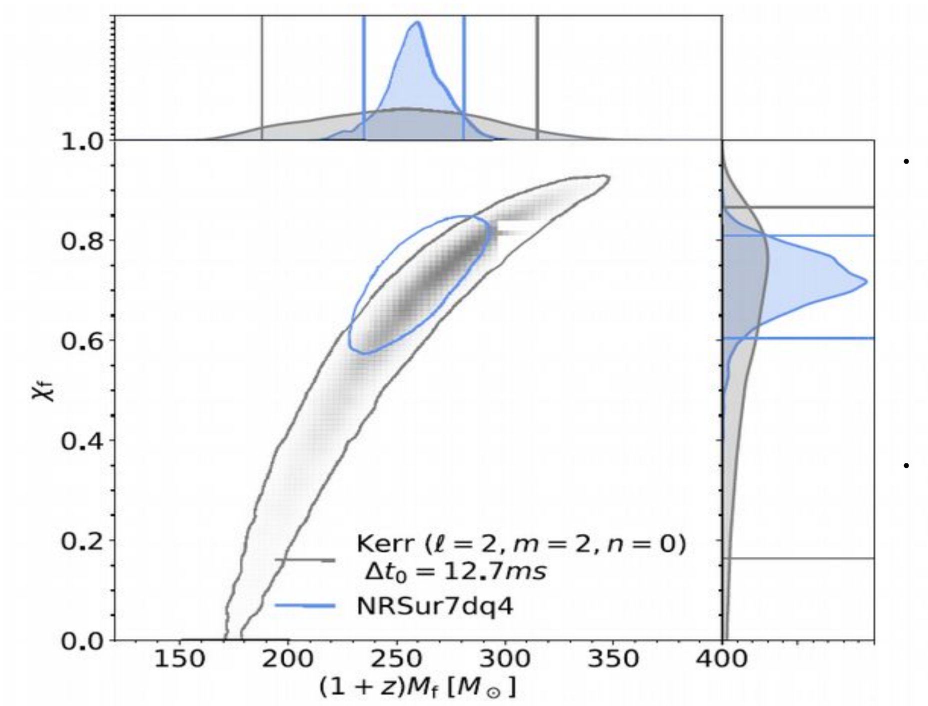

Redshifted remnant mass and spin inferred from the least-damped mode. Blue: 90% credible region of the prediction from the full-waveform analysis.

- Ringdown part of the signal has been analysed using a damped sinusoid mode; analysis estimates $f = 66^{+4}_{-3}$Hz and damping time τ 19^{+9}_{-7m}s, inferring the final redshifted mass and dimensionless spin to be $(1+z)M_f = 252^{+63}_{-64} M_\odot$ and $\chi_{f=}0.65^{+0.22}_{-0.48}$
- Results are consistent with the full-waveform analysis, the remnant ringdown signal is compatible with the full waveform analysis and GR

Signal reconstructions are obtained through a templated analysis (LALinference) and two signal-agnostic analyses (CWB and BayesWave). Reconstructions are in agreement: overlap between the CWB point estimate and the maximum-likelihood NRSur7dq4 template is 0.89, overlap between the median BayesWave waveform and the maximum likelihood NRSur7dq4 template is 0.93.

Interferometers networks near future

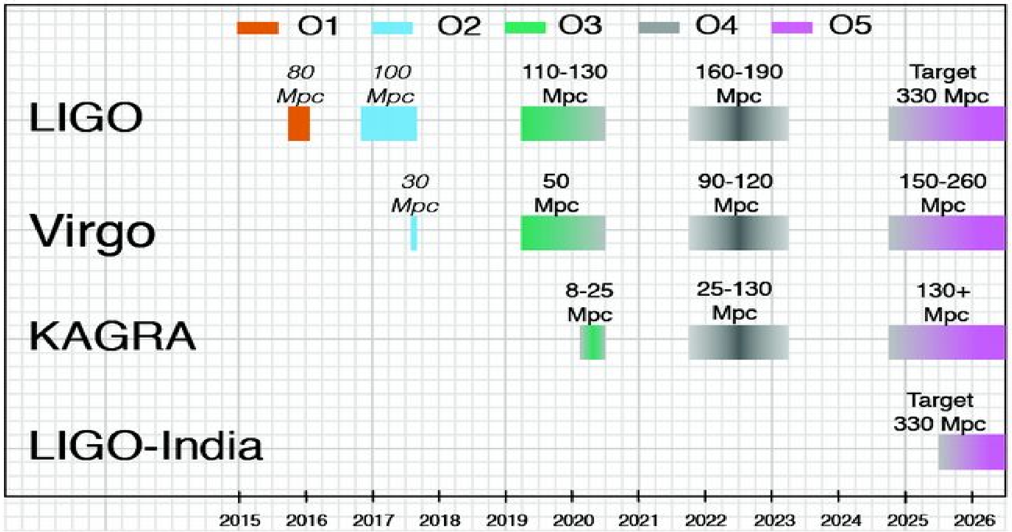

Living Reviews in Relativity 23, 3 (2020)

2022 O4: four-detector network

Late 2024/Early 2025 – 2026 O5: O5 will begin with a four-detector network incorporating the A+ upgrade for the aLIGO instruments and the AdV+ Phase 2 upgrade for Virgo.

Hardware update (Frequency independent squeezing, newtonian noise subtraction, improved coatings) will allow improvement in spectral sensitivity (low and high frequency)

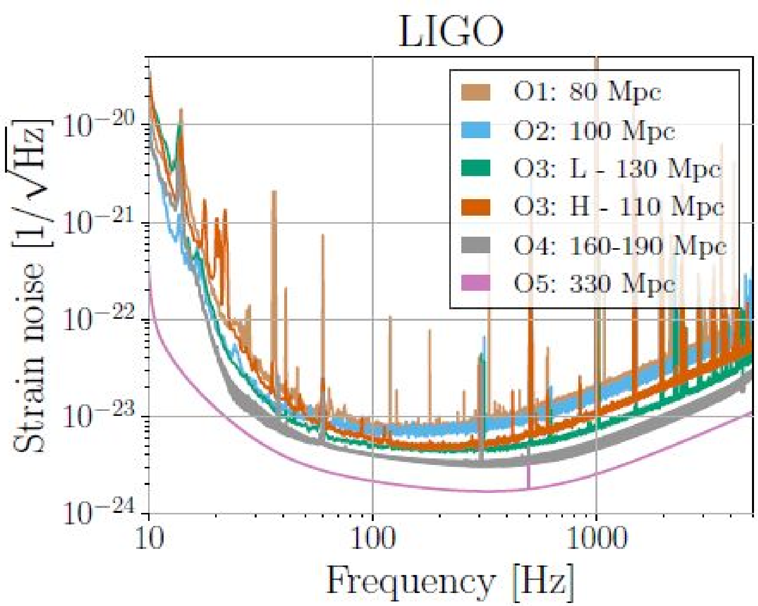

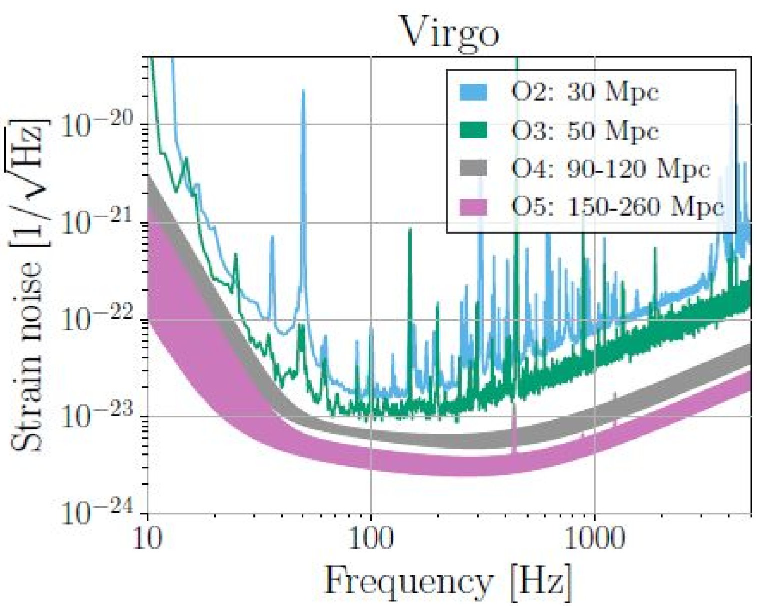

Interferometers networks future

Einstein Telescope:
- underground,
- 10-km arm triangle: multiple co-located detectors (polarization sensitivity)
- Co-located band-specific instruments (wider sensitive band)

Cosmic explorer:
40 km arm ground-based

arXiv:1912.02622v4

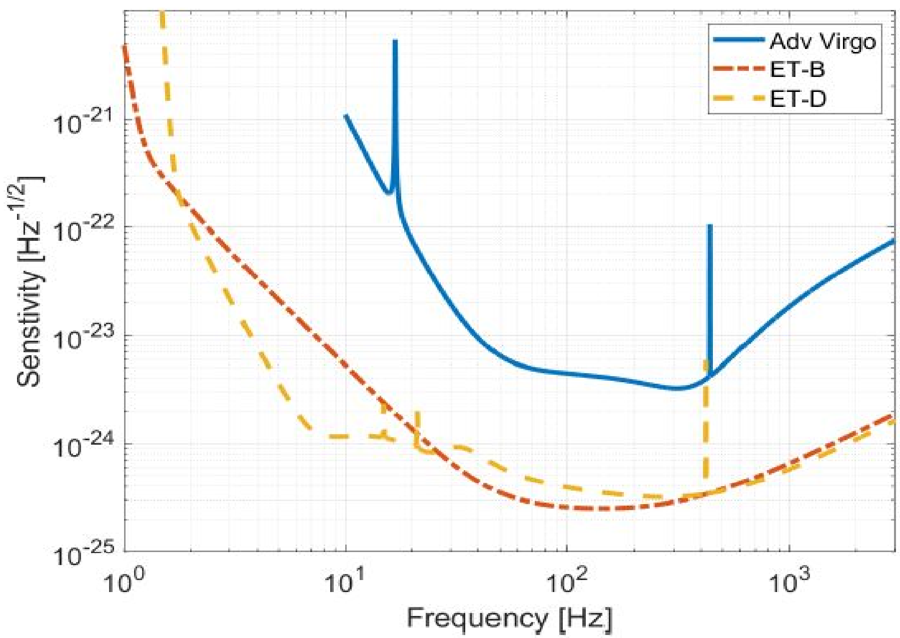

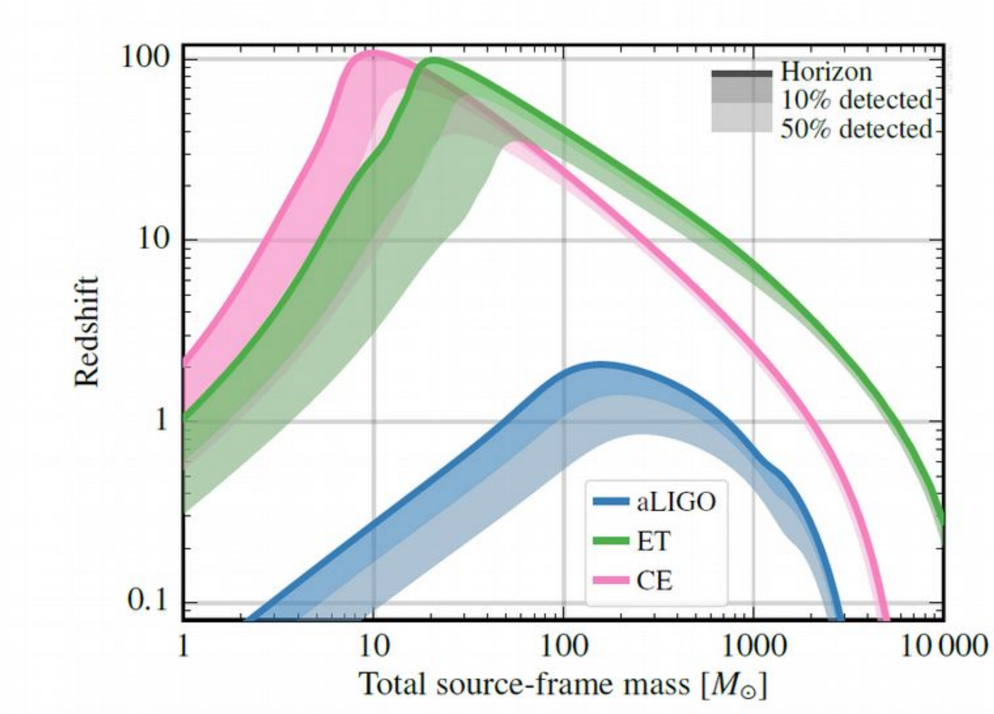

Among the potential GW science:
- strong field tests of general relativity
- testing the black hole (BH no-hair theorem, horizon structure, echoes) and black hole properties
- Neutron star properties: interior structure, EOS

Conclusions

- O1 O2 and O3: GW discoveries and many interesting signals reported
- theoretical modelling of waveform GN expected signals for binary systems coalescences have been fundamental to search for and infer properties
- GWCT-2 on O3 will be published soon

Back up